Journal of Computer-Aided Molecular Design, 10 (1996) 293–304
ESCOM

J-CAMD 347

Distributed automated docking of flexible ligands to proteins: Parallel applications of AutoDock 2.4*

Garrett M. Morris, David S. Goodsell, Ruth Huey and Arthur J. Olson**

Department of Molecular Biology, MB-5, The Scripps Research Institute, 10550 North Torrey Pines Road, La Jolla, CA 92037, U.S.A.

Received 25 January 1996
Accepted 30 March 1996

Keywords: Inhibitor; Receptor; Simulated annealing; Drug design

Summary

AutoDock 2.4 predicts the bound conformations of a small, flexible ligand to a nonflexible macromolecular target of known structure. The technique combines simulated annealing for conformation searching with a rapid grid-based method of energy evaluation based on the AMBER force field. AutoDock has been optimized in performance without sacrificing accuracy; it incorporates many enhancements and additions, including an intuitive interface. We have developed a set of tools for launching and analyzing many independent docking jobs in parallel on a heterogeneous network of UNIX-based workstations. This paper describes the current release, and the results of a suite of diverse test systems. We also present the results of a systematic investigation into the effects of varying simulated-annealing parameters on molecular docking. We show that even for ligands with a large number of degrees of freedom, root-mean-square deviations of less than 1 Å from the crystallographic conformation are obtained for the lowest-energy dockings, although fewer dockings find the crystallographic conformation when there are more degrees of freedom.

Introduction

Current computational techniques for docking of ligands to macromolecular targets [1–3] fall into two general classes. The first class might be termed 'unbiased': these techniques start the system in a random position and use a particular search engine to explore the energy landscape, searching for optimal solutions. These search engines include simulated annealing (SA), molecular dynamics and genetic algorithms. The second class might be termed 'directed': these techniques find a set of likely binding loci on the target, typically the sites of hydrogen bonding or steric complementarity, and then attempt to match the constellation of loci with the geometry of the ligand. LUDI [4] and DOCK [5] are two successful examples. The 'directed' methods have the advantage of speed, but the disadvantage of incorporating a subjective threshold: one must decide which sites are important and which are not. The 'unbiased' methods often require more computation, but make few assumptions about the potential energy landscape, and thus may find solutions missed by directed approaches.

The program AutoDock is an example of an 'unbiased' method, combining an SA conformational search engine with a rapid grid-based energy evaluation method. AutoDock predicts optimal modes of interaction of a flexible small molecule with a rigid macromolecular target. Since first described [6], AutoDock has been used in the prediction of substrate binding to enzymes [7], in computer-aided drug design of non-peptide inhibitors of HIV-1 protease [8,9] and, in a clever variation, in the docking of two proteins [10].

We describe here the new release: AutoDock 2.4. The program has been rewritten in portable ANSI C and both the techniques of coordinate manipulation and the techniques of energy evaluation have been enhanced. Profiling

*The AutoDock 2.4 suite is written in ANSI C, and is supplied with Makefiles for the following platforms: Convex, DEC Alpha OSF/1, Hewlett–Packard Precision Architecture, Silicon Graphics, and Sun. The AutoDock suite of programs is freely available to the noncommercial scientific community and to educational establishments. Further information, including additional figures and MPEG animations showing all docked conformations for each test system, can be found at the following URL: http://www.scripps.edu/pub/olson-web/doc/autodock.

**To whom correspondence should be addressed.

has helped to identify slower portions of the code, which have been subsequently optimized to increase performance. We have also developed a simple, Unix-based mechanism to launch or 'distribute' multiple docking jobs on a 'meta-cluster' of heterogeneous workstations, and to collect and analyze the results afterwards. We have tested AutoDock 2.4 on a variety of experimentally determined, structurally known complexes, having ligands of increasing complexity and number of degrees of freedom. These systems were chosen to test a variety of binding modes: ligands which bind chiefly due to hydrophobicity, to a combination of electrostatics and hydrophobicity, to chiefly electrostatic interactions, and to mainly hydrogen bonds. In the cases of benzamidine binding to β-trypsin and camphor binding to cytochrome P-450$_{cam}$, we were able to achieve 100% success in reproducing the crystal conformation using a clustering tolerance of 1.5 Å root-mean-square deviation (rmsd).

Materials and Methods

In any docking scheme, two conflicting requirements must be balanced: the desire for a robust and accurate procedure and the desire to keep the procedure computationally feasible. The AutoDock technique combines a positional, orientational and conformational search engine with a grid-based method of energy evaluation. AutoDock 2.4 supports the SA search technique, although 3.0 also incorporates a hybrid genetic algorithm and local search engine [11]. Simulated annealing allows a reasonably large number of degrees of freedom to be searched during the docking experiment, but it is not guaranteed to find the global minimum conformation. The grid-based technique provides a detailed energetic model at reasonable computational cost, but carries with it the restriction of a rigid protein target. The SA docking technique has been previously described [6] and in application to the substrates of aconitase [7]. Here, we focus on enhancements to the reported algorithms.

In discussing the docking protocols, it is necessary to define some commonly used terms. A docking *job* is a single process instantiated by one command typed at the UNIX prompt, and controlled by a single docking parameter file. Each job's parameter file may specify several independent dockings or *runs*. Each run is begun with the ligand in a specific location and conformation, operates on this one instantiation of the ligand and arrives, finally, at a docked conformation. After all the requested runs have been performed, cluster analysis is carried out on the docked conformations. In each run of SA, a prescribed number of *cycles* are carried out, each cycle maintaining a constant annealing temperature, but successively reduced as the run progresses. During each cycle, the conformation and location of the ligand are changed to generate new states for each of these changes: the ligand is said to have made a move or a *step*. This step may be either *accepted* or *rejected* depending upon the annealing temperature, the new state's energy and its previous energy [6].

Random initialization and maximum allowable initial energy

The ligand molecule is allowed to explore the six spatial degrees of freedom, for orientation and translation, and a ligand-specific number of torsional degrees of freedom. We shall refer to the complete set of variables which defines the ligand's conformation as its state variables, or 'state' for short. The user may choose to start the molecule in a particular conformation and location, or to have each new docking run begin at a random state. In order to remove any bias in the automated docking procedure, the ligand may begin at a randomly chosen state, using the argument 'random'. However, placing the ligand purely at random within a grid can accidentally cause some or all of its atoms to clash sterically with the receptor. During a subsequent SA run, typical values of the maximum translational step size may limit the ligand to making moves which are also all within the receptor, trapping it within the small interstices of the protein. The result is a continual series of unproductive rejections and a final docked energy of 10^5 kcal mol^{-1} or more. To obviate such situations, the parameter 'e0max' was introduced. If a randomly chosen initial state has an energy that exceeds this criterion, then new random states are generated until this condition is satisfied. This mode of initialization may take a long time when the volume of the low-energy regions of the grid approximately equals the volume of the ligand, and the ligand is highly flexible: in such situations a less-stringent 'e0max' value may be necessary. The user may also set a limit to the maximum number of retries. If the energy criterion cannot be satisfied within this number of retries, then the state with the minimum energy found during re-initialization is chosen as the starting point for docking. This energy criterion eliminates random starts where the initial position of the ligand sterically clashes with the receptor, and helps to place the ligand in the solvent space.

Coordinate manipulation

In many search procedures, random changes to states must be generated and evaluated. In AutoDock, each new state is generated by adding or subtracting a random fraction of a maximum step size for each state variable, then converted into Cartesian coordinates, and then into a pseudo-energy is evaluated. The maximum step size can be reduced geometrically at the end of each annealing cycle, by multiplying by a constant between 0 and 1. Alternatively, the user may specify the starting and ending values and have AutoDock calculate the correct factor based on the number of requested SA cycles.

TABLE 1
EQUILIBRIUM RADIUS AND WELL-DEPTH PARAMETERS FOR AutoGrid AND AutoDock 2.4

Atom type	van der Waals		Hydrogen bond	
	r_{eqm} (Å)	ε (kcal mol^{-1})	r_{eqm} (Å)	ε (kcal mol^{-1})
C	2.00	0.15	–	–
P	2.10	0.20	–	–
N	1.75	0.16	1.90	5.0
O	1.60	0.20	1.90	5.0
S	2.00	0.20	2.50	1.0
H	1.00	0.02	–	–

The new coordinates are generated by applying torsion rotations (if any) to the original input coordinates first. Then the rigid-body rotation and translations are applied. This way the vectors representing the rotatable bonds need not be recalculated at every step. There is an added advantage that accumulated rounding errors are avoided, which would accrue if each change were applied relative to the state's previous coordinates.

Changes to torsional degrees of freedom are applied in order from the leaves to the root of the branching torsion tree. An auxiliary program called AutoTors has been written to assist the definition of rotatable bonds in the ligand. Bond lengths and bond angles are not allowed to vary over the course of the simulation.

We have found the quaternion formulation to be the most robust method for modeling rigid-body orientations [12,13]. The original Eulerian formulation suffered from 'gimbal lock' at low values of the second angle, with the result that at some orientations large changes in angular values were needed to make small changes in actual orientation. Quaternions allow more intuitive control of a ligand's rigid-body orientation and eliminate such angular displacement singularities. Quaternions may be conveniently thought of as an axis in space, with an associated rotation about this axis. At any given step during a simulation, the orientation of the ligand is defined by a single quaternion transformation, which transforms the torsion-modified original input coordinates. Random changes in orientation are achieved by multiplying the current quaternion by a second, random, quaternion transformation. The latter consists of a random axis, and a small random rotation applied about this axis. In practice, random x-, y-, and z-components of this axis are chosen independently, so the distribution of perturbation vectors is only approximately spherically symmetric.

Translations are straightforward; a random translational step is applied in the x-, y-, and z-directions at each time step. Once again, each new state is generated with respect to the original starting coordinates, to avoid rounding errors. A problem occurs at the boundary of the search space, however. When the ligand encounters a face of the grid-map volume, a two-dimensional diffusive movement often occurs, similar to that proposed for a molecule encountering a protein surface. Often, the ligand spends a significant portion of the simulation time wastefully exploring this artificial surface. To resolve this problem, a reflective barrier was introduced. If a given translational step causes the ligand to intersect an energetic wall, twice the opposite translation is applied. This serves to 'bounce' the ligand away from faces and edges, back into the relevant portions of the state space.

Energy evaluation

We have implemented a grid-based method to precalculate grid maps of pairwise atomic interaction energies, similar to those reported by Pattabiraman et al. [14] and Goodford [15]. The protein target is placed in a three-dimensional grid, and a probe atom systematically visits each grid point. For each grid point the pairwise interaction energy of the probe is summed over all protein atoms within a nonbonded cutoff radius of 8 Å, and stored. The final grid of energies provides a lookup table for the rapid evaluation of interaction energies. Separate grids are calculated for each type of atom in the ligand, including a dispersion/repulsion term and, if appropriate, a hydrogen-bonding energy. A separate electrostatic-potential grid is calculated, and is discussed in more detail below. These grids are read into memory at the start of the docking job, then sampled by the ligand's atoms using trilinear interpolation.

The AutoDock force-field parameters are a subset of those of AMBER [16]. For a given probe atom, i, and all protein atoms, j, within a nonbonded cutoff distance, R_{cut}, van der Waals [17] energies are calculated using a traditional Lennard-Jones 12–6 potential:

$$E_{vdW} = \sum_{i<j, R_{ij}<R_{cut}} \left(\frac{A_{ij}}{R_{ij}^{12}} - \frac{B_{ij}}{R_{ij}^{6}} \right)$$

where R_{ij} is the distance between interacting atoms. The coefficients A_{ij} and B_{ij} are calculated from well depths, ε, and equilibrium contact distances, r_{eqm}, of homogeneous pairs. Table 1 shows the parameters used in AutoGrid and AutoDock 2.4. Combining rules are geometric for well-depth, and arithmetic for contact distance:

$$\varepsilon_{XY} = \sqrt{\varepsilon_{XX}\varepsilon_{YY}}$$

$$r_{eqm,XY} = \tfrac{1}{2}(r_{eqm,XX} + r_{eqm,YY})$$

where X and Y denote different atom types. Assuming that the potential is a minimum at r_{eqm} with a value of $-\varepsilon$, then:

$$A_{ij} = \varepsilon_{XY}\, r_{eqm,XY}^{12}$$

$$B_{ij} = 2\varepsilon_{XY}\, r_{eqm,XY}^{6}$$

The van der Waals coefficients used in this study are derived from the values shown in Table 1. These differ in small details from the coefficients reported earlier.

Hydrogen bonds are treated with a traditional 12–10 potential:

$$E_{H\text{-bond}} = \sum_{i<j, R_{ij}<R_{cut}} \left(\frac{C_{ij}}{R_{ij}^{12}} - \frac{D_{ij}}{R_{ij}^{10}} \right)$$

Coefficients C_{ij} and D_{ij} may similarly be calculated for hydrogen bonds using the assumption of minimum energy, $-\varepsilon$, at internuclear separation, r_{eqm}, thus:

$$C_{ij} = 5\varepsilon_{XY}\, r_{eqm,XY}^{12}$$
$$D_{ij} = 6\varepsilon_{XY}\, r_{eqm,XY}^{10}$$

We have obtained good results using an artificially strengthened hydrogen-bonding potential, with well-depths increased by a factor of 10, as described in an earlier paper [6]. The hydrogen-bond parameters used in this study are also included in Table 1.

In addition to the atomic affinity grid maps, AutoDock requires an electrostatic-potential grid map. Partial atomic charges have to be assigned to the macromolecule. The electrostatic grid can be generated by AutoGrid, or by other programs such as MEAD* [18,19] or DELPHI** [20] which solve the linearized Poisson–Boltzmann equation [21]. AutoGrid calculates electrostatic-interaction-energy grid maps using a Coulomb potential, either with a user-defined constant dielectric or with a screened Coulomb potential of Mehler and Solmajer [22]. The latter uses a sigmoidal distance-dependent dielectric function:

$$\varepsilon(r) = A + \frac{B}{1 + ke^{-\lambda Br}}$$

where: $B = \varepsilon_0 - A$, with $\varepsilon_0 = 78.4$ (the dielectric constant of bulk water at 25 °C), $A = -8.5525$, $k = 7.7839$, and $\lambda = 0.003627$ Å^{-1}, are parameters taken from Ref. 22. Electrostatic-potential grids are calculated with a probe carrying a single positive charge. The electrostatic interaction energy of each atom in the ligand is obtained by multiplying the trilinearly interpolated electrostatic potential taken from this grid with the partial charge of the atom.

Intramolecular interaction energies are also calculated for the ligand at each time step. Dispersion/repulsion and hydrogen-bond energies are monitored using the above functional forms. Internal electrostatic energies are calculated using a distance-dependent dielectric constant of $4r_{ij}$, removing a square-root calculation for each nonbonded atom pair from each time step. It is important to choose simple functional forms for the internal energy calculation, as these are calculated at every time step, instead of once during the grid precalculation for intermolecular energies.

Constraints

We have now implemented constraints for ligand translations, for rotatable bonds, and for a distance-constrained pair of nonbonded atoms in the ligand. Translational constraints are implicitly determined by the extents of the grid maps. The ligand may not attain a translation that takes any of its atoms outside the grid. If this happens, the ligand rebounds as described earlier.

AutoDock 2.4 supports two kinds of torsion constraints, one 'soft' and the other 'hard'. Soft constraints are specified by the preferred torsion angle and the constraint's half-width, which are used to define an inverted-Gaussian energy profile. At the preferred angle the energy is zero, but increases to the barrier energy further away. By contrast, a hard torsion constraint keeps torsion angles exactly within the user-defined bounds, and does not allow the torsion angle to deviate from these bounds.

A distance constraint has been introduced for nonbonded atoms: this requires that for every conformation generated, the flagged distance be calculated and checked for constraint violation; if outside the allowed distance range, the step is rejected, no energy calculation is performed, and a new state is generated.

User interface

The AutoDock 2.4 user interface is more intuitive than the previously reported version, with the introduction of a keyword parser and a command mode. In the interactive setup program AutoTors, the user picks rotatable torsion angles, and decides if nonpolar hydrogen atoms should be merged: AutoTors then writes out the ligand input file for AutoDock. Input for AutoGrid and AutoDock is keyword-based, allowing easy modification of parameters. AutoDock also has a command mode, which can be used to calculate energies for arbitrary conformations, to return the energy of a state specified by state variables alone, and to convert trajectories of states into stacked frames of Cartesian coordinates. We have created many auxiliary Unix scripts to assist in setting up AutoDock jobs, and in subsequent analysis of the results. These are particularly useful when combining the results of distributed jobs, and performing cluster analysis on these grouped results.

The new keyword-based interface of AutoDock 2.4 now accepts pairwise interaction-energy parameters either as coefficients and exponents, or as equilibrium separation, well-depth and exponents. The latter form is new and somewhat more intuitive. It is also possible to specify the starting and ending values for translation, quaternion and torsion-angle step sizes and have the parser calculate the correct per-cycle reduction factors for each.

*MEAD is available from Donald E. Bashford, Dept. Molecular Biology, Mail Drop MB-1, The Scripps Research Institute, 10666 North Torrey Pines Road, La Jolla, CA 92037, U.S.A.

**DELPHI is available from Biosym Technologies, 9685 Scranton Road, San Diego, CA 92121-2777, U.S.A.

TABLE 2
X-RAY CRYSTAL-STRUCTURE COORDINATES USED IN DOCKING EXPERIMENTS

Protein/ligand complex	PDB entry	Resolution (Å)	Number of torsions in ligand	Reference
β-Trypsin/benzamidine	3ptb	1.7	0	23
Cytochrome P-450$_{cam}$/camphor	2cpp	1.63	0	24
McPC-603/phosphocholine	2mcp	3.1	4	25
Streptavidin/biotin	1stp	2.6	5	26
HIV-1 protease/XK263	1hvr	1.8	10	27
Influenza hemagglutinin/sialic acid	4hmg	3.0	10	28

Cluster analysis

Analysis of docking results is accomplished by 'structure binning'. The docked conformations are first sorted in order of increasing energy. The coordinates of the lowest-energy conformation are compared by rmsd with those of all other conformations, and grouped into the same cluster if the rmsd is less than the user-defined rmsd threshold. This comparison process is repeated until all conformations have been clustered. A list of families of similar, docked conformations is produced, ranked from lowest to highest energy. If known, a 'reference' structure can be specified, for example the X-ray crystal structure observed by experiment. The rmsd between each docked conformation and the reference structure can then be calculated, thus giving a measure of the success of the docking.

Symmetry checking, which, e.g., treats the three symmetry-related rotations of a *tert*-butyl group as equivalent, is optional in the rmsd calculation. For the current atom in the comparison structure, the squared distance is calculated to all atoms with the same atom type in the reference structure, and the minimum value assigned to the current atom. This is repeated for all atoms in the comparison structure, and the square root of the mean of these minimum values is calculated. This simple algorithm for symmetry checking works correctly when the two conformations are similar, but can break down when the conformations are significantly different, giving spuriously low rmsd values. We have not used the symmetry checking in the rmsd calculations presented here.

Distributed docking

The dockings described here were performed using a 'cluster' of Hewlett–Packard Precision-Architecture 9000/735 workstations. The cluster, which is just a list of host names, was defined by a script which identified the nodes with the lowest loads. The cluster can consist of a list of heterogeneous architectures, as long as AutoDock has been compiled for each. Scripts were generated by a small utility called 'makelaunch', to launch the dockings on the cluster, and to group the results of the docking. The grouping script concatenates all the available docked conformations that have been output by the running or completed AutoDock jobs. AutoDock can be run with a clustering parameter file, which specifies amongst other things, this grouped file, the clustering rmsd tolerance and a reference structure such as an experimentally determined structure. AutoDock outputs the conformations into clusters ranked by energy. This output can be visualized by software such as AVS, during and at the end of the distributed docking runs.

Test systems and docking protocols

Two sets of experiments were performed. The first set was designed to test AutoDock's ability to predict binding modes in a representative variety of ligand–protein situations. The second set of docking experiments explored the effects of changing different SA parameters on a particular docking's outcome.

For the first set of experiments, six systems [23–28] listed in Table 2 were chosen to test the enhancements of AutoDock. We chose problems with a range of dimensionality, from 6 to 17 degrees of freedom (translation, rigid-body orientation and torsions, if any). Crystallographic coordinates were taken from the Brookhaven Protein Data Bank, and the ligand and protein atoms separated into different files. For the ligand, all hydrogen atoms were added in the SYBYL molecular modeling package*. Partial atom-centered charges were evaluated where possible by the semi-empirical approach of MOPAC using the MNDO Hamiltonian; SCF charges were calculated: neither Mulliken nor electrostatic potential (ESP) charges were derived. When the ligand's number of atoms exceeded the capacity of MOPAC, empirical charges were assigned using the Gasteiger method. Hydrogen atoms bonded to a carbon were then deleted and their charges added to that of the carbon, yielding a 'united atom' model. The protein was treated in a slightly different way: after removing all waters, polar hydrogens were added in SYBYL, and charges assigned using the Kollman united-atom library. It was necessary to resolve ambiguities in the positions of polar hydrogens on tyrosines, threonines and serines: we used 'pol_h' (David

*SYBYL is available from Tripos Associates, Inc., 1699 South Hanley Road, Suite 303, St. Louis, MO 63144-2913, U.S.A.

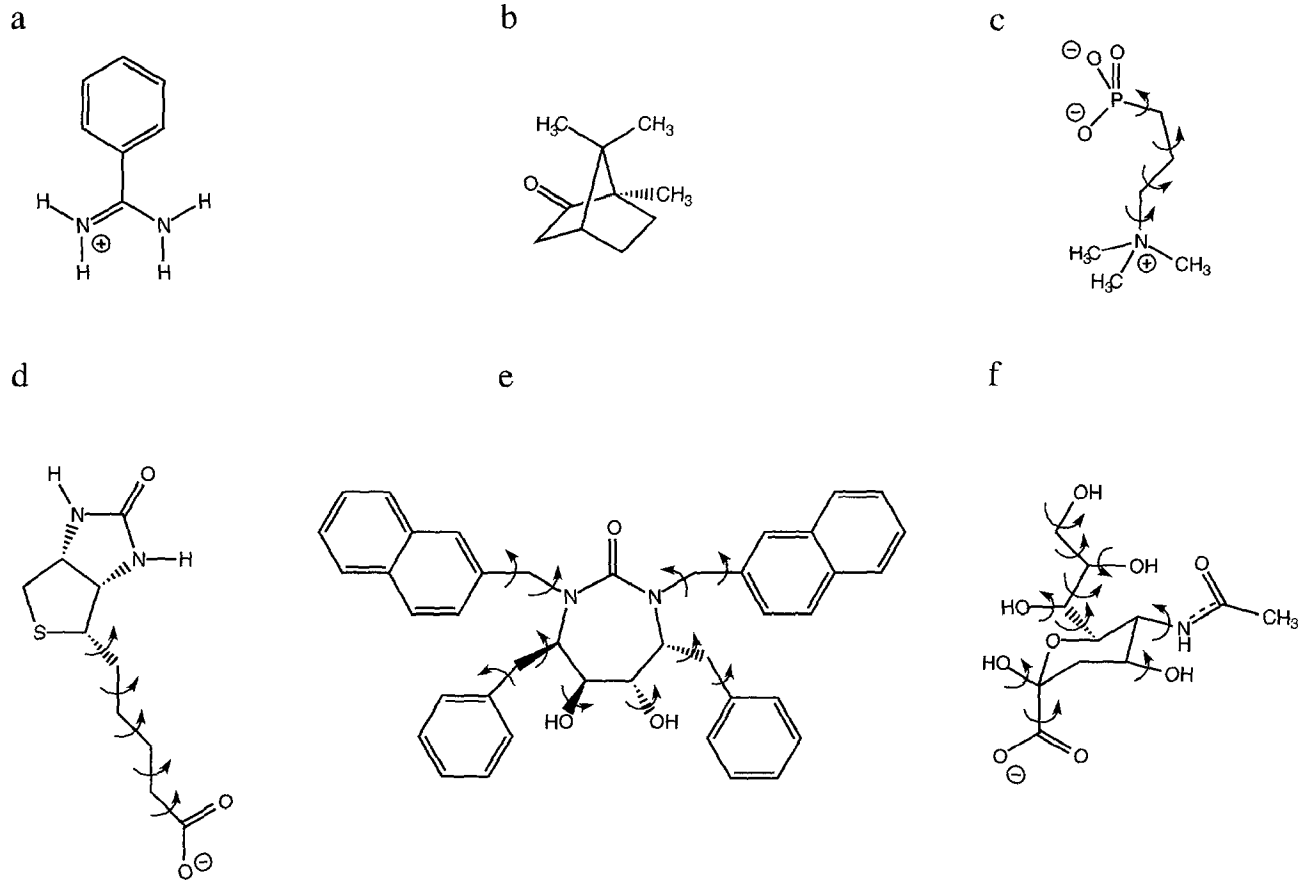

Fig. 1. The ligands chosen for docking, with rotatable bonds highlighted: (a) benzamidine; (b) camphor; (c) phosphocholine; (d) biotin; (e) HIV-1 protease inhibitor XK-263; and (f) sialic acid.

Case, personal communication) to achieve improved placement over the default locations assigned by SYBYL, and HBPLUS 3.0 [29] to place lysine polar hydrogens. In cytochrome P-450$_{cam}$ [24], the default position of Tyr^{96} hydroxyl hydrogen added by SYBYL created a steric clash with the hydrogen HG1 of Thr^{101}. The former hydrogen was manually repositioned so as to relieve this clash, but retained a coplanar position with the phenyl ring. Atomic affinity and electrostatic grids were calculated from the resulting polar-hydrogen protein models using AutoGrid.

For every test case considered, a grid spacing of 0.375 Å was used, centered on the active site of the protein and with 61 points in each Cartesian direction, thus making a total of 226 981 points per grid. Hence, the grid dimensions in all cases were 22.875 Å × 22.875 Å × 22.875 Å. The 'active site' in each case was defined knowing where the ligand bound: the aim here was to investigate if SA could reproduce the experimentally observed X-ray crystal structure.

The systems chosen for testing are listed in Table 2, and shown in Fig. 1. One hundred docking runs were performed in each case, distributed evenly among 10 Hewlett–Packard Precision Architecture 9000/735 workstations. At the beginning of each SA run, the ligand began with a random translation, random quaternion and where present, random torsions. Each run consisted of 50 annealing cycles. A cycle terminated if the ligand made 25 000 accepted moves, or 25 000 rejected moves, whichever came first. The annealing temperature, RT, was 616 cal mol^{-1} during the first cycle, and was reduced linearly at the end of each cycle. The state with the minimum energy found during the current cycle was used to start the next cycle. For all the test systems studied here, the initial cycle and final cycle translational maximum step sizes were 3.0 and 0.2 Å, respectively, and for the rigid-body orientation and torsion angles, the initial and final maximum step sizes were 24° and 5°, respectively. The energy of the crystal conformation of the ligand was calculated using 'epdb' in the command mode of AutoDock.

The second set of experiments was designed to investigate the choice of SA parameters and their effect on the outcome of a particular ligand/receptor docking run. The first column of Table 5 shows the parameters used. This testing regimen was applied to benzamidine docking to β-trypsin. The first and second sets of four experiments were identical, except that the first set used the minimum-energy state from the previous cycle, while the second used the last state. The third set of experiments investigated

dockings with schedules of increasing length. The final set investigated the effect of doing more docking runs.

Results

The results of the first set of docking experiments with the six test systems are shown in Fig. 2 and summarized in Table 3. In those cases where more than one conformational cluster was found, the energy of the second-lowest energy cluster of conformations gave a measure of the specificity of the technique: in all cases except sialic acid/hemagglutinin, the best solution was energetically well-separated from the less-favorable conformations. Figure 3 shows a comparison of the population of each cluster found, using an rmsd clustering tolerance of 1.5 Å.

Benzamidine/β-trypsin (3ptb)

One of the simplest systems tested was benzamidine binding to β-trypsin. Benzamidine contains a hydrophobic benzyl ring attached to a polar amidine and binds tightly in the specificity pocket of trypsin [23]. We treated the amidine moiety as protonated. There were no torsional degrees of freedom owing to delocalization of the π-electron cloud, so the ligand was docked as a rigid body. The 'e0max' keyword was used with an argument of 0.0 kcal mol^{-1}, to ensure that no runs began with a positive energy. As can be seen from Table 3, 100% of the docked conformations found the crystallographic conformation. The top-ranked, i.e. lowest-energy, docked conformation had an rmsd of 0.23 Å, and an energy of about 4 kcal mol^{-1} lower than that of the crystal structure (see Fig. 2a). This was probably due to close contacts of the amidine hydrogens, which were not modeled in the crystallographic refinement. Interestingly, the lowest energy conformation was also the one with the lowest rmsd from the crystallographic conformation.

Camphor/cytochrome P-450$_{cam}$ (2cpp)

The binding of camphor to cytochrome P-450$_{cam}$ is dominated by hydrophobic interactions and a single hydrogen bond that is donated from the Tyr^{96} hydroxyl to the carbonyl oxygen of camphor. Camphor is a fused-ring system, so it was docked as a rigid body. Using a clustering rmsd tolerance of 1.5 Å, 100% of the camphor dockings were clustered into the same rank. However, this cluster contained two subclusters (of which the mean energies were almost identical) that could be distinguished with a tolerance of 0.5 Å. The two clusters had almost identical mean energies: one contained 76 members and matched the crystallographic conformation (the lowest rmsd was 0.29 Å; see Fig. 2b), while the other contained 24 members and placed the carbonyl oxygen in the correct hydrogen-bonding position, but rotated the cage-like body of the molecule by 180°. This latter subcluster had crystallographic rmsd values of about 0.4 Å higher than the top-ranked subcluster. Furthermore, all 100 docked conformations had energies lower than that of the crystal. The lowest energy structure found had an rmsd from the crystallographic coordinates of 0.95 Å. The oxygen-affinity grid map helped to orient the camphor, reproducing the observed hydrogen bond between the P-450$_{cam}$ Tyr^{96} hydroxyl and the camphor carbonyl oxygen. The unusually high energy for the crystallographic coordinates was dominated by a positive energy for camphor's oxygen (see Table 3), which again may be due to crystallographic refinement without explicit hydrogens.

Phosphocholine/Fab McPC-603 (2mcp)

The binding of phosphocholine to the Fab McPC-603 is an example that is predominantly electrostatic in character. Phosphocholine was treated with four rotatable bonds. As can be seen from Table 3, the cluster with the lowest energy consisted of 15 of the dockings, each of which found the crystallographic conformation. This

TABLE 3
RESULTS OF SIMULATED-ANNEALING DOCKING

PDB entry	Number in rank 1	Energy (kcal/mol) and rmsd from observed crystal structure (Å)						Energy of crystal structure (kcal/mol)
		Lowest energy rank 1	Rmsd rank 1	Energy of lowest rmsd	Rmsd of lowest rmsd	Lowest energy rank 2	Rmsd rank 2	
3ptb	100	−51.01	0.23	−51.01	0.23	N/A[a]	N/A[a]	−47.27
2cpp	100[b]	−36.95	0.95	−36.01	0.29	N/A[a]	N/A[a]	9.05[c]
2mcp	15	−33.50	0.96	−33.50	0.96	−28.18	6.76	8.53[d]
1stp	35	−52.98	0.89	−50.38	0.50	−42.46	1.79	−26.56
1hvr	4	−76.69	0.86	−76.17	0.72	−51.51	5.43	−99.79
4hmg	5	−25.14	1.40	−23.74	1.27	−24.65	3.10	−24.31

In the SA 100 runs, 50 cycles, 25 000 accepted, 25 000 rejected steps per cycle were used. The rmsd clustering tolerance was 1.5 Å.

[a] Not applicable, since only one conformational cluster was found.

[b] This cluster could be further classified into two subclusters using a more stringent clustering tolerance of 0.5 Å, the lower-energy cluster containing 24 members.

[c] The crystal conformational energy was dominated by the high intermolecular nonbonded energy of camphor's O, (39.65 kcal mol^{-1}).

[d] The crystal conformational energy was dominated by an internal bad contact (2.26 Å apart) in phosphocholine, between C2 and O1.

cluster was also the most populated (see Fig. 3). Note also that the lowest energy in cluster rank 1 was some 5 kcal mol^{-1} lower than the lowest energy in cluster rank 2. The conformation with the lowest energy was −51 kcal mol^{-1}. The lowest rmsd from the crystal coordinates was 0.23 Å (see Fig. 2c). As was the case with benzamidine docking to β-trypsin, the lowest energy docked conformation was also the one with the lowest rmsd from the crystal structure.

Biotin/streptavidin (1stp)

The streptavidin–biotin complex [26] is one of the most tightly binding complexes known, with an experimentally observed dissociation constant K_d of 10^{-15} M. This high affinity results from several factors, including the formation of multiple hydrogen bonds and van der Waals interactions between biotin and the protein, along with the ordering of surface polypeptide loops that bury the biotin in the protein interior. We once again made the assumption that the induced fit had already occurred in the protein, and proceeded to dock biotin to the complexed protein conformation. Biotin has five rotatable bonds, and with more torsional degrees of freedom than the earlier examples, represented a more challenging docking. The energy of the crystal conformation of biotin was about −27 kcal mol^{-1}, while the lowest energy found by SA docking was about −53 kcal mol^{-1}, having an rmsd of 0.89 Å. The best rmsd found was 0.50 Å, with an energy of about −50 kcal mol^{-1} (see Fig. 2d). Figure 3 shows that the top-ranked cluster was clearly the most populated.

XK-263/HIV-1 protease (1hvr)

The HIV-1 protease provides a particularly challenging target for automated-docking techniques used in computer-aided drug design. The substrates and inhibitors of HIV-1 protease are typically extended peptides or peptidomimetics, with a dozen or more freely rotatable bonds. When bound, they are completely enclosed within an active-site 'tunnel'. Presumably, the protease opens up in vivo, allowing the continuous polypeptide chain to insert into the active site, which is then embraced by closing of the flaps. Most current docking protocols, however, use a rigid protein target, disallowing the opening and closing of gates. The substrate must either 'thread' its way into the active site, or an assumption must be made to place the substrate into the active site. The cyclic urea HIV-protease inhibitor XK-263 [27] has 10 rotatable bonds, if we exclude the cyclic-urea's flexibility. Since there are considerable energy barriers at the ends of the active-site tunnel which the inhibitor must surmount, the initial annealing temperature was raised a 100-fold in this particular case. The 'e0max 0.0' command was not used here, because initialization took too long: this is a good example of a highly constrained binding pocket with a large flexible ligand. Out of the 100 dockings, 4% of the conformations were clustered into the top rank, which matched the crystal conformation. The lowest energy conformation had an rmsd of 0.86 Å, and the best conformation had an rmsd of 0.72 Å from the crystal coordinates (see Fig. 2e). It is worth noting that of all the test systems, only in this instance did the SA fail to find an energy

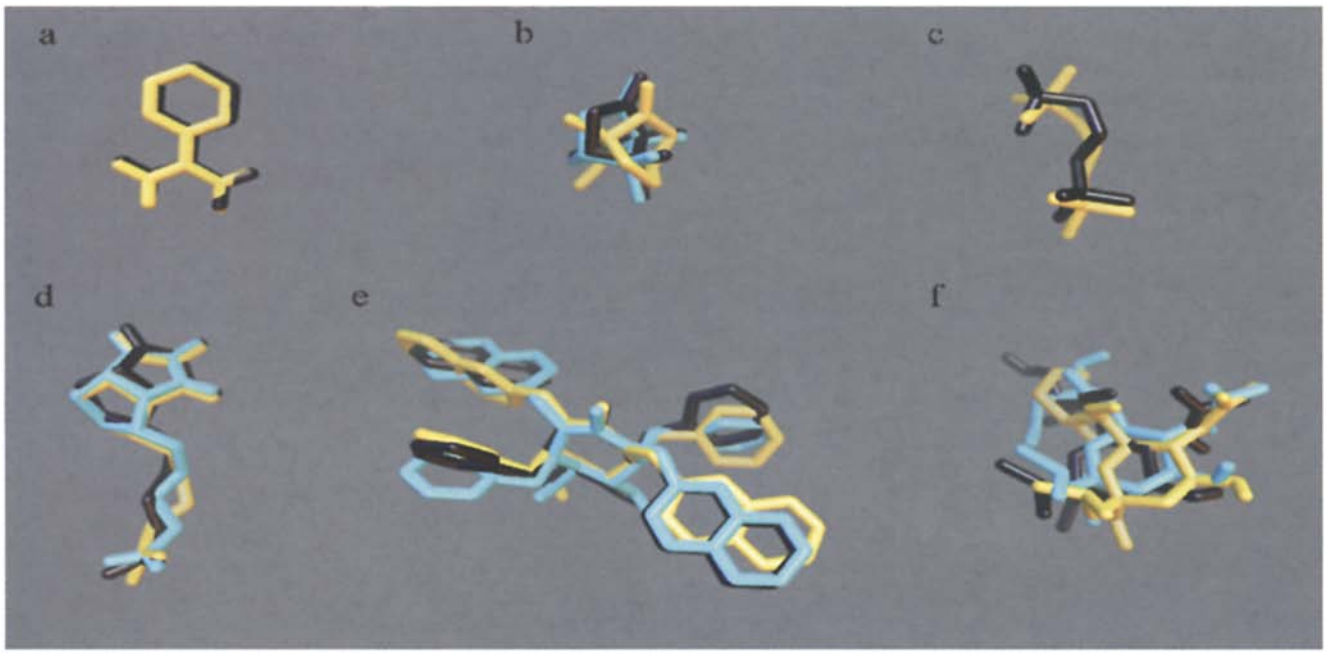

Fig. 2. Results of the six docking test cases: crystallographic coordinates are black, the lowest-energy docked conformation is yellow, and the docked conformation with the lowest rmsd from the crystal coordinates is blue. (a) The docked and crystallographic conformations of benzamidine binding to β-trypsin. (b) Camphor binding to cytochrome $P\text{-}450_{cam}$. (c) Phosphocholine binding to McPC-603. (d) Biotin binding to streptavidin. (e) XK263 binding to HIV-1 protease. (f) *iso*-Propylated sialic acid binding to influenza hemagglutinin.

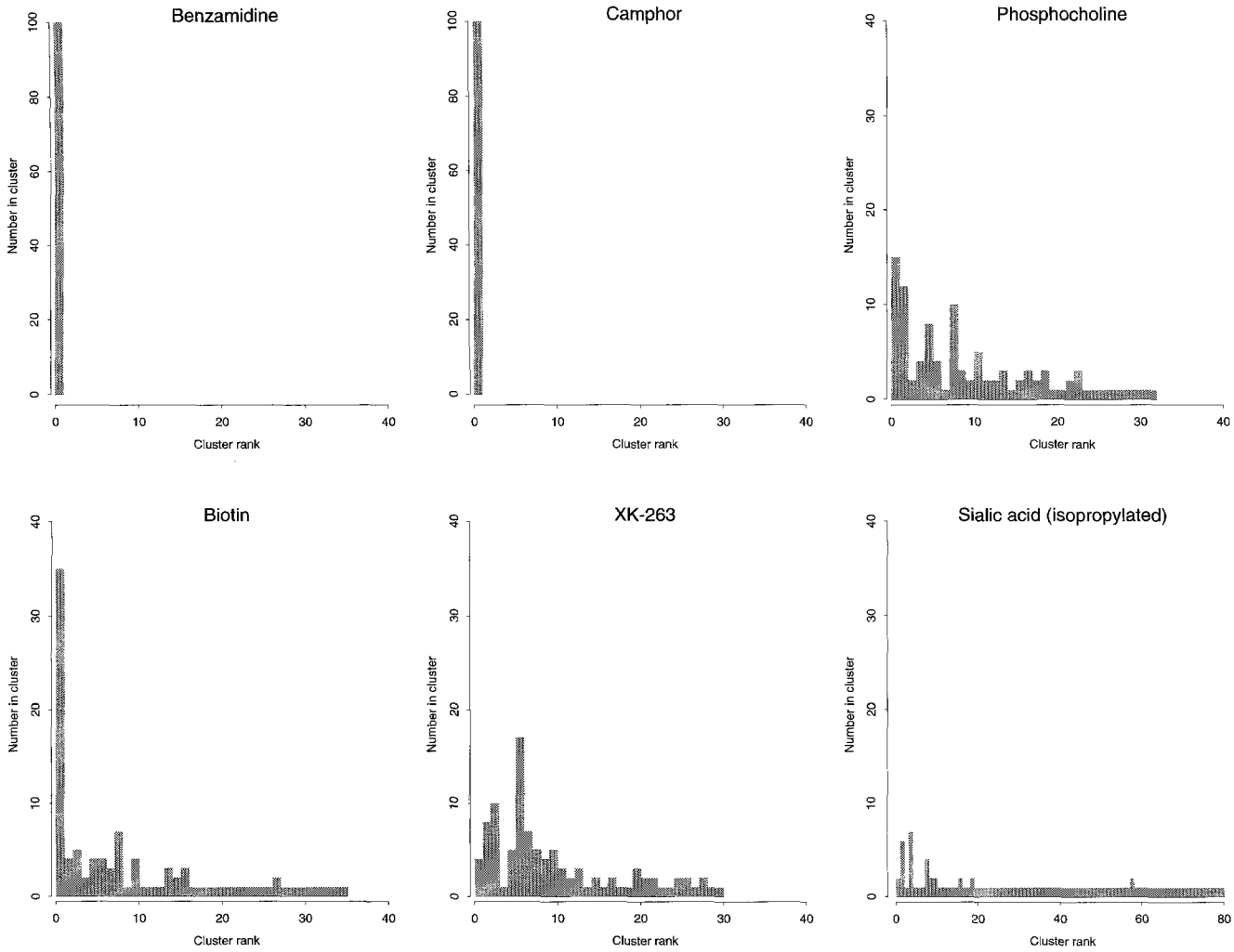

Fig. 3. Results of the six docking test cases: number of conformations found in each conformationally similar cluster, versus cluster rank. These clusters were obtained using an rmsd clustering tolerance of 1.5 Å. The clusters are ranked from lowest energy (rank = 1) to highest. Note that at this tolerance, only one cluster was found for benzamidine and camphor.

lower than that of the crystal. The lowest energy found was −76.69 kcal mol^{-1}, compared with that of the crystal structure, which was −99.79 kcal mol^{-1}. Using the 'epdb' command (which gives a detailed breakdown of the total energy) in the AutoDock's command mode, we found that the chief reason for this difference with respect to the crystal conformation, was due to the increased intramolecular energy caused by the slightly closer positions of the XK-263 aromatic side chains to its cyclic urea moiety, and an increased intermolecular energy caused by a bad contact between the XK-263 C78 and the protein.

Sialic acid/hemagglutinin (4hmg)

The binding of sialic acid to a pocket of conserved amino acids in the influenza virus hemagglutinin is dominated by hydrogen bonding. Sialic acid carries five hydroxyls (three in its glycerol moiety), one carboxylate, a cyclic oxygen, and an acetamido group, with a total of 10 rotatable bonds. It is thus possible to bind to hemagglutinin using many different combinations of hydrogen bonds. Only one mode is observed in the crystal structure. Out of 100 runs, the top-ranked cluster had five docked conformations which matched the crystallographic structure: the lowest-energy one had an rmsd of 1.40 Å, while the lowest rmsd was 1.27 Å (see Fig. 2f). The many possible pairings of hydrogen bonds yielded a wide range of different, less-favorable solutions. It is worth noting that none of the carbon atoms in the skeleton of sialic acid are within optimal van der Waals contact with any atoms of the protein; this shows that, as one might expect, the majority of binding enthalpy is provided by the bristling hydrogen-bonding groups.

Timings

All dockings were carried out on a cluster of 10 Hewlett–Packard Precision-Architecture 9000/735 workstations. Performance data for a single SA run are given in Table 4, averaged over 10 runs; this table shows the

TABLE 4
PERFORMANCE FOR A SINGLE SA DOCKING RUN

Docking run	Mean number of steps per run	Mean CPU usage per run (s)
3ptb	1 723 843	354.71
2cpp	1 819 903	360.83
2mcp	1 549 397	369.60
1stp	1 812 038	878.70
1hvr	1 728 403	1569.07
4hmg	1 778 968	1121.38

The mean total number of accepted plus rejected steps versus mean CPU usage, running on a Hewlett–Packard Precision-Architecture 9000/735 workstation are shown. The schedule parameters were 10 runs, 50 cycles, maximum of 25 000 accepted steps, maximum of 25 000 rejected steps, and select the state with the minimum energy from the previous cycle.

mean total number of accepted plus rejected steps, and the mean CPU usage time. The schedule parameters were 10 runs, 50 cycles, maximum of 25 000 accepted steps, maximum of 25 000 rejected steps, using the state with the minimum energy from the previous cycle. Although not explicitly shown in this table, the time taken to complete all 100 runs was the same as that to complete 10 runs, since they were distributed among the 10 workstations.

Schedule experiments

The results of the series of experiments designed to study the effects of the SA parameters upon the docking's outcome are summarized in Table 5. There are a number of points of interest here. The first is that the methodology of starting the current cycle with the *last* state of the previous temperature cycle, is not as effective as taking the *minimum* state. Another intriguing point is that increasing the number of cycles while keeping the total maximum number of steps constant (at 2.5 million), the success of the docking decreases using the minimum state, but increases using the last state. Success here can be measured by several criteria: (i) the lowest energy found; (ii) the highest energy found; (iii) the lowest rmsd found; and (iv) the percentage of docking runs with an rmsd from the crystallographic coordinates of less than 1.0 Å. It is also worth noting that when the number of steps per cycle was reduced a 100-fold, from {10, 50, 25 000, 25 000, m} to {10, 50, 250, 250, m}, the lowest energy found was still very close to the crystallographic conformation; however the proportion of runs with docked rmsd values of less than 1.0 Å dropped from 80% to 10%. Thus for this particular example, benzamidine docking to β-trypsin, a shorter schedule would have sufficed. The schedule {10, 50, 250 000, 250 000, m} was the only schedule for which all of the docked structures showed an energy less than that of the crystallographic complex and rmsd values of less than 1.0 Å. However, the schedules with fewer steps, such as the schedule {10, 50, 25 000, 25 000, m}, still find solutions close to the crystallographic structure in ~80% of the cases, but at a reduced computational cost.

TABLE 5
RESULTS OF SIMULATED-ANNEALING SCHEDULE EXPERIMENTS ON BENZAMIDINE AND β-TRYPSIN

Schedule parameters[a]					Energy (kal/mol) and rmsd (Å)						Runs with rmsd < 1 Å (%)
					Lowest energy	Rmsd	Highest energy	Rmsd	Lowest rmsd	Rmsd	
10	50	25 000	25 000	m	−50.13	0.34	−28.28	7.97	−49.19	0.23	90
10	500	2500	2500	m	−51.28	0.57	−26.17	11.34	−50.09	0.44	70
10	5000	250	250	m	−50.80	0.21	−19.34	13.38	−50.59	0.20	30
10	50 000	25	25	m	−33.36	3.24	−12.45	9.61	−33.36	3.24	0
10	50	25 000	25 000	l	−20.17	9.11	7.36	11.79	−7.56	7.21	0
10	500	2500	2500	l	−31.60	4.44	−16.20	9.49	−31.60	4.44	0
10	5000	250	250	l	−51.41	0.46	−7.33	15.12	−47.72	0.24	40
10	50 000	25	25	l	−50.77	0.39	−19.60	8.00	−50.77	0.39	20
10	50	25	25	m	−21.83	5.41	−9.43	9.28	−21.83	5.41	0
10	50	250	250	m	−46.27	0.39	−10.41	8.89	−46.27	0.39	10
10	50	2500	2500	m	−49.63	0.60	−21.96	10.64	−49.60	0.47	30
10	50	25 000	25 000	m	−49.97	0.44	−27.31	8.91	−49.05	0.24	80
10	50	250 000	250 000	m	−49.95	0.36	−48.10	0.45	−49.11	0.27	100
10	50	25 000	25 000	m	−50.31	0.37	−34.22	3.96	−50.31	0.37	80
50	50	25 000	25 000	m	−50.91	0.55	−24.46	11.21	−49.76	0.19	90
100	50	25 000	25 000	m	−51.32	0.53	−24.41	11.54	−48.56	0.13	88
500	50	25 000	25 000	m	−51.33	0.53	−26.43	8.47	−49.01	0.09	89.6

[a]Schedule parameters are respectively: number of runs; number of cycles; maximum number of accepted steps; maximum number of rejected steps; selection for next cycle, where 'm' = minimum energy and 'l' = last state from previous cycle. All rmsd values are calculated with respect to the observed crystal conformation. No symmetry checking was used. Note that the crystal-structure energy was −47.27 kcal mol^{-1}.

Conclusions

Simulated annealing is a relatively powerful search technique for solving a variety of NP-complete problems. Although not proven here, we assert that flexible molecular docking falls into this category of so-called 'hard' problems. Our results show that SA performs remarkably well with small- to medium-sized ligand-docking experiments, with up to about eight torsional degrees of freedom. Higher-dimensional problems benefit from the increased state-space sampling afforded by distributed docking. A significant advantage of the distributed docking technique is that it does not depend upon access to parallel supercomputers: the temporal benefits of parallelization can be achieved using networked Unix workstations. Direct interprocess communication is unnecessary: the grouping script, which is run on the local host, collects the docked results together for a local instantiation of AutoDock to perform cluster analysis.

We have found that exploiting SA to the fullest sometimes requires several dockings with different schedules and starting conditions, although the method of starting the current cycle with the minimum-energy state from the previous cycle is superior to that of using the last state. Using the same schedule across all test systems reproduced the crystallographic conformation more frequently in systems with lower dimensionality. In other words, a similarly successful docking would have been achieved using a shorter schedule of {10, 50, 250, 250, m} for benzamidine docking to β-trypsin, as would have using {10, 50, 25 000, 25 000, m} for sialic acid docking to hemagglutinin.

In the cases considered here, the cluster of similar conformations with the lowest energy corresponded to the crystallographic mode of binding. However, in this cluster the conformation of lowest energy was not always the conformation with lowest rmsd from the crystallographic conformation: often, the rmsd of the lowest energy was 0.1–0.2 Å worse. It is therefore advisable to consider an ensemble of clustered, low-energy docked conformations.

Larger ligands with more degrees of freedom, of the order of 10 or more torsions, have proven more difficult to dock successfully with the 'standard' schedule used here, {100, 50, 25 000, 25 000, m}. We conclude that in such cases, it is necessary to utilize as much 'knowledge' of the system as is experimentally justifiable. This may require placing the ligand within the putative active site prior to docking, limiting its translational freedom, and applying torsion constraints. The ability to constrain a specific internal distance between flexible portions of the ligand has proved useful in docking a protein loop to an antibody (Ed Moret, personal communication). By constraining the two ends of the flexible model peptide to remain close to one another, the antibody's loop form was retained while allowing considerable local flexibility. We have found torsion constraints particularly helpful in docking larger, highly flexible ligands. This requires knowledge of the conformational characteristics of the ligand, which may be inferred from experimental evidence or, if unavailable, a variety of exhaustive and/or artificial-intelligence-based [30] conformational search procedures, such as COBRA*.

The 'divide-and-conquer' strategy has also been shown to be successful in applying SA docking to larger ligands [31]. This approach involves docking just a fragment of the molecule first, then freezing or constraining that conformation and adding another flexible fragment, incrementally building up to a final docked conformation. In some problems it is vital to include specific side-chain motion in order to model induced fit and to reproduce experimentally observed results [31]. It will therefore be necessary to include protein flexibility into the flexible docking approach.

To address even larger problems, we have recently incorporated a hybrid global–local search engine into AutoDock, using a genetic algorithm combined with a local minimizer [11]. We have had encouraging results in early trials using this hybrid algorithm, with indications that it requires fewer energy evaluations than SA. Future work will investigate the validity of the hybrid genetic algorithm and local search approach to flexible ligand docking.

Acknowledgements

The authors would like to thank Eric Peterson for running the schedule-comparison docking experiments. This publication number 9789-MB was supported under the National Institutes of Health Grant numbers GM48870-01 and RR08065.

References

1 Blaney, J.M. and Dixon, J.S., Perspect. Drug Discov. Design, 1 (1993) 301.
2 Kuntz, I.D., Meng, E.C. and Shoichet, B.K., Acc. Chem. Res., 27 (1994) 117.
3 Rosenfeld, R., Vajda, S. and DeLisi, C., Annu. Rev. Biophys. Biomol. Struct., 24 (1995) 677.
4 Böhm, H.-J., J. Comput.-Aided Mol. Design, 6 (1992) 593.
5 Kuntz, I.D., Blaney, J.M., Oatley, S.J., Langridge, R. and Ferrin, T.E., J. Mol. Biol., 161 (1982) 269.
6 Goodsell, D.S. and Olson, A.J., Proteins Struct. Funct. Genet., 8 (1990) 195.
7 Goodsell, D.S., Lauble, H., Stout, C.D. and Olson, A.J., Proteins Struct. Funct. Genet., 17 (1993) 1.
8 Lunney, E.A., Hagen, S.E., Domagala, J.M., Humblet, C., Kosinski, J., Tait, B.D., Warmus, J.S., Wilson, M., Ferguson, D., Hupe,

*COBRA v. 3.2 is available from Oxford Molecular Ltd., Magdalen Centre, Oxford Science Park, Sandford-on-Thames, Oxford, OX4 4GA, U.K.

D., Tummino, P.J., Baldwin, E.T., Bhat, T.N., Liu, B. and Erickson, J.W., J. Med. Chem., 37 (1994) 2664.
9 Vara Prasad, J.V.N., Para, K.S., Ortwine, D.F., Dunbar Jr., J.B., Ferguson, D., Tummino, P.J., Hupe, D., Tait, B.D., Domagala, J.M., Hunblet, C., Bhat, T.N., Liu, B., Guerin, D.M.A., Baldwin, E.T., Erickson, J.W. and Sawyer, T.K., J. Am. Chem. Soc., 116 (1994) 6989.
10 Stoddard, B.L. and Koshland, D.E., Nature, 358 (1992) 774.
11 Hart, W.E., Ph.D. Thesis, University of California, San Diego, CA, at 'ftp://ftp.cs.sandia.gov/pub/papers/wehart/thesis.ps.gz'.
12 Maillot, P.-G., In Glassner, A.S. (Ed.) Graphics Gems, Academic Press, New York, NY, 1990, pp. 498–515.
13 Watt, A. and Watt, M., Advanced Animation and Rendering Techniques – Theory and Practice, ACM Press, New York, NY, and Addison-Wesley Publishing Company, Wokingham, U.K., 1992.
14 Pattabiraman, N., Levitt, M., Ferrin, T.E. and Langridge, R., J. Comput. Chem., 6 (1985) 432.
15 Goodford, P.J., J. Med. Chem., 28 (1985) 849.
16 Weiner, S.J., Kollman, P.A., Case, D.A., Singh, U.C., Ghio, C., Alagona, G., Profeta Jr., S. and Weiner, P., J. Am. Chem. Soc., 106 (1984) 765.
17 Van der Waals, J.H., Lehrbuch der Thermodynamik, Part 1, Mass and Van Suchtelen, Leipzig, Germany, 1908.
18 Bashford, D. and Gerwert, K., J. Mol. Biol., 224 (1992) 473.
19 Bashford, D. and Karplus, M., Biochemistry, 29 (1990) 10219.
20 Gilson, M.K. and Honig, B., Nature, 330 (1987) 84.
21 Honig, B. and Nicholls, A., Science, 268 (1995) 1144.
22 Mehler, E.L. and Solmajer, T., Protein Eng., 4 (1991) 903.
23 Marquart, M., Walter, J., Deisenhofer, J., Bode, W. and Huber, R., Acta Crystallogr., Sect. B, 39 (1983) 480.
24 Poulos, T.L., Finzel, B.C. and Howard, A.J., J. Mol. Biol., 195 (1987) 687.
25 Padlan, E.A., Cohen, G.H. and Davies, D.R., Ann. Immunol. (Paris), Sect. C, 136 (1985) 271.
26 Weber, P.C., Ohlendorf, D.H., Wendolski, J.J. and Salemme, F.R., Science, 243 (1989) 85.
27 Lam, P.Y.S., Jadhav, P.K., Eyerman, C.J., Hodge, C.N., Ru, Y., Bacheler, L.T., Meek, J.L., Otto, M.J., Rayner, M.M., Wong, Y., Chang, C.-H., Weber, P.C., Jackson, D.A., Sharpe, T.R. and Erickson-Viitanen, S., Science, 263 (1994) 380.
28 Weis, W.I., Bruenger, A.T., Skehel, J.J. and Wiley, D.C., J. Mol. Biol., 212 (1990) 737.
29 McDonald, I.K. and Thornton, J.M., J. Mol. Biol., 239 (1994) 777.
30 Leach, A.R., Prout, C.K. and Dolata, D.P., J. Comput.-Aided Mol. Design, 4 (1990) 271.
31 Friedman, A.R., Roberts, V.A. and Tainer, J.A., Proteins Struct. Funct. Genet., 20 (1994) 15.